THE BALTIC JOURNAL
OF ROAD AND BRIDGE ENGINEERING

2012
7(2): 160–168

INVESTIGATION OF GEOGRID APERTURE SIZE EFFECTS ON SUBBASE-SUBGRADE STABILIZATION OF ASPHALT PAVEMENTS

Tuba Sert[1]✉, Muhammet Vefa Akpınar[2]

Dept of Civil Engineering, Karadeniz Technical University, Kanuni Campus, Trabzon 61080, Turkey
E-mails: [1]tsert16@hotmail.com; [2]mvakpinar70@yahoo.com

Abstract. The increased use of geogrids in highway pavement subbase layer reinforcement applications has resulted in a need to better understand the soil–geogrid interface properties for the use in analysis and design. For this purpose, a series of laboratory large scale pullout tests was carried out with three different aperture size geogrid samples randomly sampled from a single manufacturer. It was found that geogrids are unique in their pullout performance within pavement subbase layer structure based on their aperture sizes. Analysis indicates a strong relationship between pullout performance and geogrid aperture size of geogrids at moderate normal stress levels. Such findings aid in selection of appropriate geogrid types for subgrade and subbase interface reinforcement purposes. Further experimental analysis was conducted to investigate the wide-width tensile test performance for the same samples used in the pullout tests in this study.

Keywords: large scale pullout test device, geogrid aperture size, wide-width tensile test, asphalt pavements, subbase-subgrade.

1. Introduction

Geogrids are the products of choice for subbase and subgrade stabilization and base reinforcement applications. Spreading of vertical loads due to heavy traffic loads is maintained by the interlock between each aggregate particles. Geogrids confine and increase the strength of subbase layers resulting in an increased long-term pavement performance. Geogrids provide reinforcement to the base and subbase aggregate layers of pavements due to their high resistance to elongation besides to their ability to interlock with the surrounding aggregates. Geogrids contribute to the long-term performance of pavement subbase layers because of their ability to confine. In recent years, the use of geogrids for soil reinforcement has increased greatly due to their high tensile modulus properties (Phanikumar *et al.* 2009).

Geogrids are used mainly in asphalt pavement road applications to provide reinforcement to the unbound subbase pavement layer and to stabilize the low bearing capacity subgrade layer. The amount of lateral movement under these two layers can be reduced greatly by providing a geogrid within the subbase pavement layer. Partial penetration of aggregate materials through the geogrid apertures results in interlock of the subbase and subgrade aggregate particles. The reinforcing system, depending on geosynthetics tensile characteristics, can minimize the vertical settlements between high quality fill material and poor foundation soils resulting in an increased road performance (Palmeira, Antunes 2010).

Geogrid type, number of geogrid layers and depth of the geogrid in the reinforced soil are important for bearing capacity of geogrid. The test results showed both qualitative and quantitative relationships between the bearing capacity and the geogrid parameters (Alamshahi, Hataf 2009). The geogrid aperture shape effects and its bearing capacity were investigated by Dong *et al.* (2010) and it was found that the triangular aperture size geogrid was more effective than the rectangular aperture size geogrid (Dong *et al.* 2011).

Geogrids are reinforcement materials with varying aperture sizes consisting of a combination of transverse and longitudinal polymer ribs. The intersection of the ribs has very high strength which prevents the lateral movement of the ribs under stress. These transverse and longitudinal ribs provide passive interface shear strength against the pullout forces (Sert, Akpinar 2011).

The soil–geosynthetic interaction mechanisms can be very complex, depending on the type and properties of the geosynthetic and the soil (Palmeira 2009). Specially, new theoretical methods related to stability of granular soils

ISSN 1822-427X print / ISSN 1822-4288 online
doi: 10.3846/bjrbe.2012.22
http://www.bjrbe.vgtu.lt

are presented in literature (Abusharar *et al*. 2009; Moraci *et al*. 2012). Pullout mechanism is closely related to geometrical grid parameters including rib spacing and transverse rib diameter (Palmeira, Milligan 1989), aggregate particle size and soil moisture content (Jewell 1990). The pullout load is usually determined as a total of the lateral bearing resistance of the geogrid ribs and the friction effect between geogrid surface and the soil (Palmeira 2004).

A lof of studies related with geogrid types and mesh geometries focused on quantifying the various pullout mechanisms (Lopes, Ladeira 1996; Sugimoto *et al*. 2001) and geogrid reinforcements (Kongkitkul *et al*. 2010; Rowe, Taechakumthorn 2011; Yeo, Hsuan 2010).

Moraci and Gioffrè (2006) compared the pullout test results conducted on the three different geogrids with the same normal stress and embeded anchorage lengths. They observed that peak interface apparent coefficient of friction of soil–geogrid interface was strongly affected by the shape geogrids geometry and applied confining stress but less affected by the geogrids longitudinal tensile stiffnesses and reinforcement length.

Teixeira *et al*. (2007) reported that soils reinforced with geogrids may indicate higher interface shear strength compared to the unreinforced soils. Palmeira (2004) showed that passive ressistance occuring in front of the geogrid decreased the pullout shear mobilization between soil and transverse ribs.

Several studies have shown that geosynthetics are effective reinforcement structural materials for long term pavement performance. Subaida *et al*. (2009) explained in their study that it was possible to reduce the base layer thickness of the pavement as long as the geosynthetic material cost was less than the base material. This is important particularly for developing countries where geosynthetics are costly. They also showed that benefits of using geosynthetic depend on the quality of the geosynthetic material and the thickness of the pavement layer. Other researchers (Montanelli, Cancelli 1999; Ghosh, Madhav 1994; Perkins 1999) have found that soil–geosynthetic interaction and subgrade strength are important parameters in reinforcement mechanisms of pavements layers.

Alagiyawanna *et al*. (2001) showed that longitudinal members contribute more resistance to pullout forces than transverse members of the geogrid. This is due to the fact that higher elongations occur in the longitudinal direction.

In this study, three types of rectangular aperture size geogrids are analysed between the pavement subbase layer and compacted subgrade layer. For this purpose, pullout tests were carried out with three different aperture size geogrid samples randomly sampled from a single manufacturer. Pullout tests and wide-width tensile tests were compared.

2. Experimental studies

2.1. Pullout tests

Pullout tests are performed in laboratory conditions to determine resistance of geogrids to pullout. The purpose is to simulate the field conditions and compare the geosynthetic material performance. A special designed large scale pullout test device built at Karadeniz Technical University, Trabzon, Turkey was utilized to perform the pullout experiments. Geogrid samples were tested under 35 kPa vertical pressures three times for repeatability purposes. All the pullout tests were performed at a displacement rate of 5.0 mm/min until the geogrid samples were ruptured. The tests were performed under displacement control of 5.0 mm/min to capture the shear strength-displacement response envelope.

The pullout test box used in the experimental program is shown in Fig. 1. The pullout test device was composed of a rigid pullout box, vertical and horizontal pistons, a clamping system and measurement sensors (pressure gauges, strain gauges that have 5000 microstrain capacity, vertical and horizantal LVDTs) and data acquisition system. Pressure gauges and strain gauges were provided by Tokyo Sokki Kenkyujo Company. Two types of pressure gauges were used for laboratory tests: 200 mm diameter and 2 MPa measurement capacity KDA-PA/KDB-PA gauge and 50 mm diameter from 200 kPa to 2 MPa measurement capacity KDE-PA/KDF-PA gauge. KM strain gauges have $\pm 5000 \times 10^{-6}$ strain measurement capacity. 100 mm, 500 mm and 1000 mm measurement capacity LVDTs were provided by TDG Company to measure the lateral and vertical displacements.

Fig. 1 shows the general view of the pullout test equipment used in this research program. The dimensions of the test-box are 1000 mm (length), 1000 mm (width), 800 mm (height). The ASTM standard *Standart Test Method for Measuring Geosynthetic Pullout Resistance in Soil* specifies the dimensions of large-scale pullout test boxes to be larger dimensions such as 610 mm long, 410 mm wide, and 300 mm high.

The pullout test device was mainly made of steel profiles that were interconnected with bolts. The loading plate and vertical piston were built to apply vertical pressures. To measure vertical displacements value, 1000 mm capacity LVDT was placed near the vertical piston.

The subgrade and subbase soils were filled from the back side of the box and was compacted after the back side was closed with the "U" profile steels. Each layer soil was compacted at 0.2 MPa stress level which was obtained from the field study under a roller compacter as shown in Fig. 2. As the the roller compacter passed over subbase layer, the 200 mm pressure gauge located on top of the layer measured the compaction stress. A 15 t force capacity horizontal piston system clamped by metal clamp was used to pullout the embeded geogrid samples. Two 500 mm capacity LVDTs, placed left and right side of the tensile apparatus, were used to measure geogrid's horizontal displacement. 24 channel data acquisition system was used during the pullout tests to record the data.

Typical pavement loads of 80 kN single axle load and 700 kPa pressure load are considered for pavement designing (Wu 2007). According to *2002 Guide for the Design of New and Rehabilitated Pavement Structures* the equivalent single axle load (ESAL) for heavy vehicles was determined as 80 kN (18000 lb) in the U.S. According to the studies of Priest *et al*. (2005), Mulungye

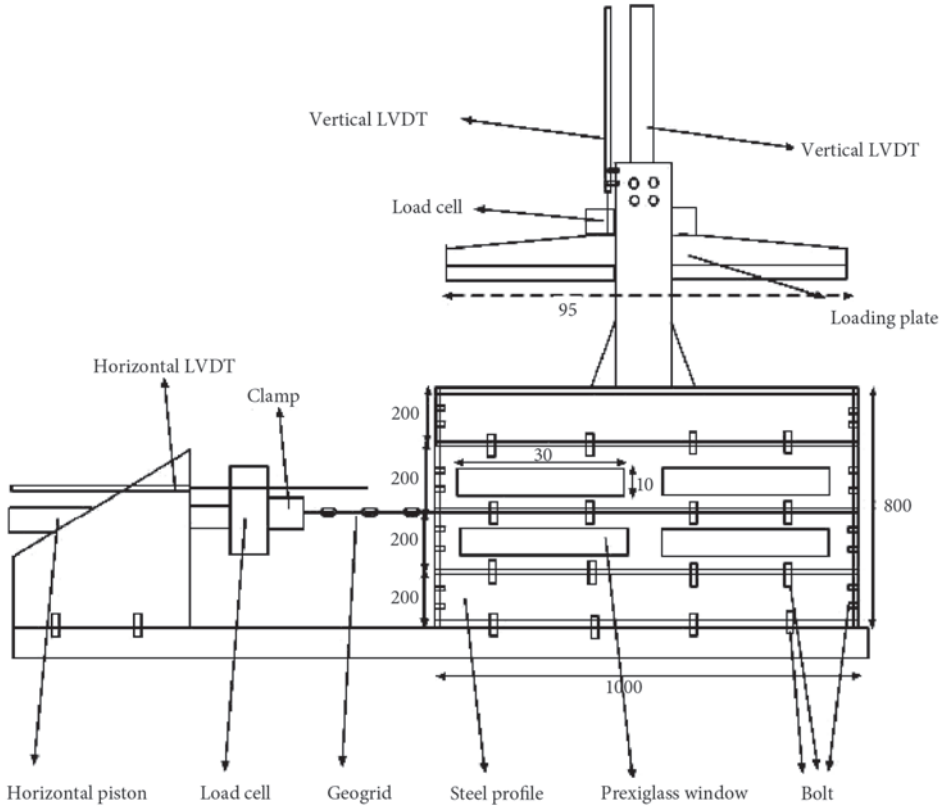

Fig. 1. Schematic view of the pullout apparatus. Not to scale and all dimensions are given in mm

et al. (2007) and Fang *et al.* (2007), the axial load of 80 kN was chosen. Park (2008) found that tire pressures on pavement ranged from 550 kPa to 890 kPa. Priest *et al.* (2005) accepted the vertical pressure on subbase layer as 35 kPa. In this study, for determining tire contact pressure, measurements were obtained in field. Heavy truck loads were measured on the field by using the 200 mm diameter pressure gauges installed on top of asphalt pavement layer and subbase layer. The measured pressures ranged from 550 kPa to 790 kPa on top of the pavement surface and from 31 to 33 kPa on top of the subbase layer. In each test, 35 kPa vertical pressure and ESAL's of 80 kN were applied during the lateral pullout force by the vertical piston in the pullout tests in accordance to the field and previous study.

Fresh specimen was randomly cut from the sample rolls of the geogrid material. Three types of biaxial

Fig. 2. 200 mm diameter pressure gauge and roller compacter compacting the subbase layer

geogrid samples randomly sampled from a bacth of their product were used in the testing program. These geogrids were 50×50 mm, 40×40 mm, and 30×30 mm aperture size geogrids as shown in Fig. 3. 50×50 mm aperture size refers to 50×50 mm. Prior to performance of the pullout tests, the geogrids were visually inspected

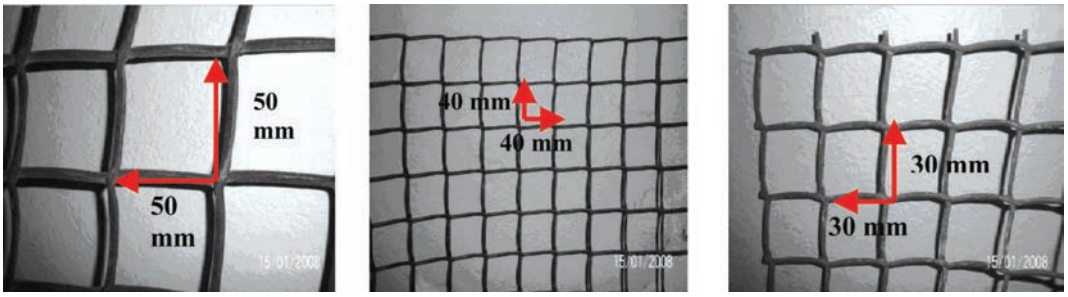

50×50 mm 40×40 mm 30×30 mm

Fig. 3. Three types of different aperture size geogrids

and no defects were found. Biaxial geogrid samples can carry loads applied in x-y directions in the plane of the geogrid.

Table 1 summarizes the properties of the subbase and subgrade soil and Fig. 4 shows the gradation curve for the two soil materials used in the tests. First, the subgrade soil was placed in the half of the box, then the geogrid wsa layed and finally the subbase material was spread and compacted. Optimum water content of subgrade material was 18% and subbase material was 4.7%.

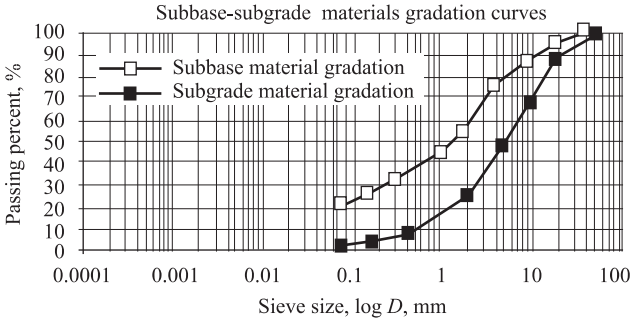

Fig. 4. Gradation curves for subgrade and subbase layer soils

Table 1. Properties of the subbase and subgrade soil used in the pullout test experiments

Property	Unit	Subgrade soil	Subbase soil
Liquid limit	%	23	–
Plastic limit	%	18	Nonplastic
Max dry unit weight	kN/m^3	18.23	19.1
Friction angle	°	27.4	34.2
Cohesion	kPa	29.21	13.4

Fig. 5. Pressure gauge and strain gauge placements on top of the subbase layer. Plan view of pressure gauge and and strain gauges

Loose granular subgrade fill material was placed in 100 mm lifts. The total fill thickness of 800 mm was maintained prior to pullout testing. The subgrade soil was initially dried (110.5 °C) and later it was compacted inside the box at a moisture content of 4.7%.

Pressure gauges with 1MPa capacity shown in Fig. 5 were located approx 70 mm above and below the geogrid samples to measure the vertical pressure distributions. The 50 mm diameter pressure gauges were aligned near to the pullout box edge. The strain gauges were placed next to the pressure cells. One big pressure cell (ø = 200 mm) with a 2 MPa capacity was positioned in the middle of the pullout box.

One of the special features of this device was the plexiglass windows on both sides of the pullout box device and the digtial image processing. 300 mm long and 150 mm plexiglass windows opened on right and left sides of the large scale pullout test box and the digital camera were used to measure the geogrid sample displacements. The pullout test device with plexiglass windows and digital image processing is the first application at literature.

The digital image method was used to quantify the lateral and vertical displacements of geogrid samples inside the box during the pullout tests. The digital image process allowed to determine the displacements on the x-y coordinates of scale meters which were placed on the plexiglass window during construction of the device. The variations of displacement of grid members in the longitudinal direction were found to be insignificant. This is due to the fact that the soil above, below and inside the geogrid aperture imposed high constraint. It is worth noting that the magnitudes of the settlements in the subbase layer were non-uniform due to the soil characteristics and the non-uniform vertical pressure distribution. The reinforced subbase was subjected to an average settlement of 20 mm.

It can be said that when geogrid ribs with varying aperture sizes are combined with a subbase aggregate, it produces a mechanically stabilised layer with no lateral (minimal) displacements. As long as high strength junctions and stiff ribs are provided with effective mechanical interlock of aggregate particles into the aperture, the permanent deformation of subbase layer is expected to result in high resistance. According to tensile tests, mechanical properties of geogrids are shown in Table 2.

Table 2. Mechanical characteristics of geogrids

Aperture dimensions	Unit	50×50 mm			40×40 mm			30×30 mm		
Test No.		1	2	3	1	2	3	1	2	3
Load (at peak value)	kN/m	5.64	5.76	5.76	2.8	2.72	2.64	3.52	2.32	3.32
Strain (at ultimate)	%	25	25.5	23	25	11	15	75	14	26
Strain (at peak value)	%	11	9	10	5	5	6	23	7.5	10
Displacement (at peak value)	mm	40	26	30	14	16	17.5	70	22	26
Displacement (at ultimate)	mm	87	75	68	76	32	45	80	43	76

2.2. Wide-width tensile test

Wide-width tensile strength experimental analysis was conducted on same geogrid samples used in the pullout testing program. For this purpose 300 mm wide and 300 mm long geogrid samples were tested under wide-width tensile test device. The wide-width tensile tests were performed on geogrids with a fixed cross-section area until the geogrids break apart. The tests showed typical plastic deformation.

3. Results and analysis

3.1. Pullout shear strength results

Pullout shear strength test results showed that the interaction between the given subbase soil and geogrid has been perfect for the pullout interface strength design of these structures. All the studied geogrid samples especially the 50×50 mm aperture size geogrid showed a higher mutual effect with the subbase soil.

Fig. 6 demonstrates the pullout strength versus displacement results under normal pressure equal to 35 kPa. As seen in Fig. 6, the 40×40 mm aperture size geogrid and 30×30 mm aperture size geogrid have shown close pullout strengths. The 30×30 mm aperture size geogrid has shown some more durability to pullout force but when it starts to rupture, it quickly looses its durability and shows less displacement than the 40×40 mm aperture size geogrid. The 50×50 mm aperture size geogrid has given ideal results of durability and displacement values. The durability which it showed until the rupture point is approximately 2 times higher than of the 30×30 mm and 40×40 mm aperture size geogrids. Just like the other geogrid versions the 50×50 mm aperture size geogrid's pullout load graphic has shown increasing inclination until the rupture point. The geogrids showed an increasing stress-strain relationship to the yield point, then failed after this point.

Mechanism of full interaction between geogrid samples and soil was obtained during the pullout tests. In this study S/D ratios (the bearing member space ratio) of 12.5, 13.3, and 10 were obtained for 50×50 mm, 40×40 mm, 30×30 mm aperture size geogrids, respectively. S is the dimensions of geogrid and D is the member thickness. These S/D values were slightly higher than in the previous study by Jewell (1990), since their geogrid samples and loading conditions were slightly different. In this study, no lateral displacements were observed on the geogrid samples indicating mechanism of full interaction. This is mainly due to the high S/D ratio of the geogrid samples. As geogrid aperture dimensions become larger, pullout strength increases. This result can be explained according to the previous studies. Study from Palmeira and Milligan (1989) indicated that the pullout strength is highly affected by S/D (the bearing member space ratio). Higher pullout strength from geogrid bearing members can be obtained as the S/D ratio increases, according to Jewell (1990). Max interface shear or mechanism of full interaction can be achieved as the S/D ratio reaches 10.

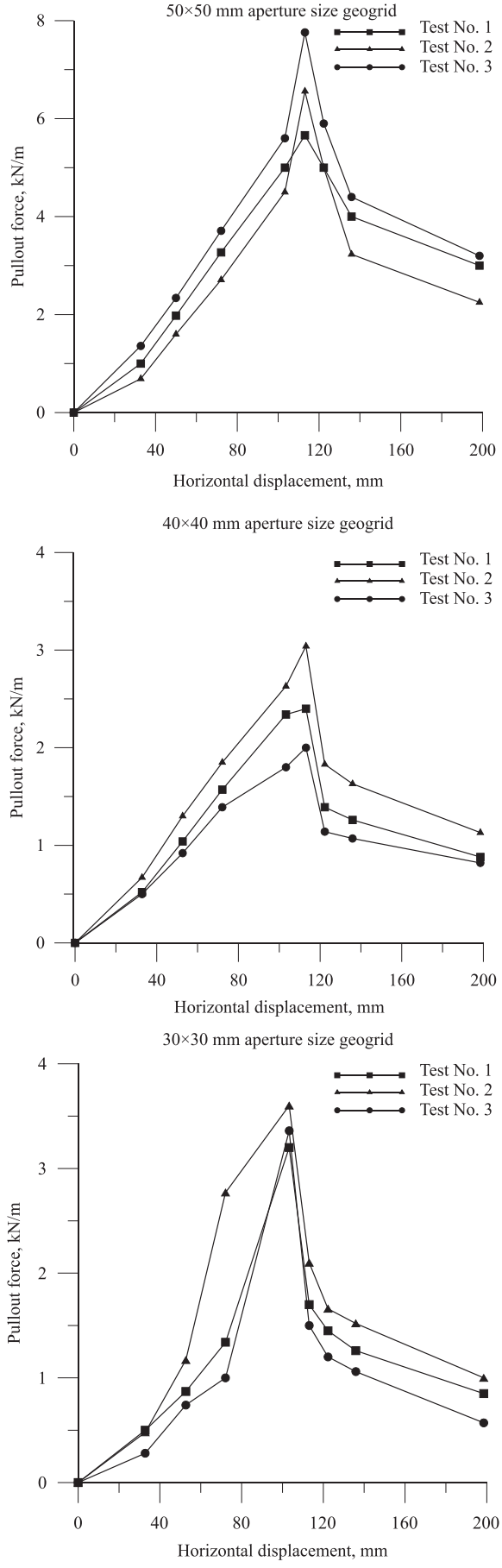

Fig. 6. Load-horizontal displacement curve from aperture size geogrids

In this study, the pullout peak strength values for all types of geogrids were calculated as 6.66 kN/m, 2.48 kN/m, 3.38 kN/m for 50×50 mm, 40×40 mm, 30×30 mm aperture size geogrids, respectively (Fig. 6). The average value can be computed as 4.17 kN/m. Similar pullout strengths were reported by Teixeira *et al.* (2007).

The digital image process indicated that the variation of displacement of the longitudinal members was found to be insignificant. As shown in Fig. 7, no lateral displacement indicates that aggregate particles are constrained within the geogrid aperture resulting in an improved subbase pavement layer performance life. It can be said that when combined with a suitable subbase aggregate geogrids with varying aperture sizes produces a mechanically stabilised layer with no lateral displacements. The high strength junctions of the apertures (no ruptures were observed) allowed strong interlock of aggregate particles.

The findings of this study demonstrated performance differences between geogrids with varying aperture sizes. It is important to note that these conclusions are based on research performed with three different aperture size geosynthetic reinforcing materials compacted between the subgrade and the subbase soil layers.

3.2. Vertical stress distribution

Table 3 summarizes the statistical analyses of stresses obtained at top and bottom of geogrid level. According to Table 3 for test number 1 the stresses measured by sensor 1, 2, 3, and 4 located at the bottom of 50×50 mm aperture size geogrid gave high standard devition stress value of 35. The average stress value was computed as 49 kPa which was almost 3 times higher than the stress value of 14 kPa. Similar trends were observed for tests number 2 and 3 which gave standard deviation values of 18.01, 12.1, respectively. For all tests and sensors of 50×50 mm aperture size geogrid at the bottom of geogrid level, it was observed that average value 36 kPa and standart deviation as 21.7. When it was compared between bottom and top of

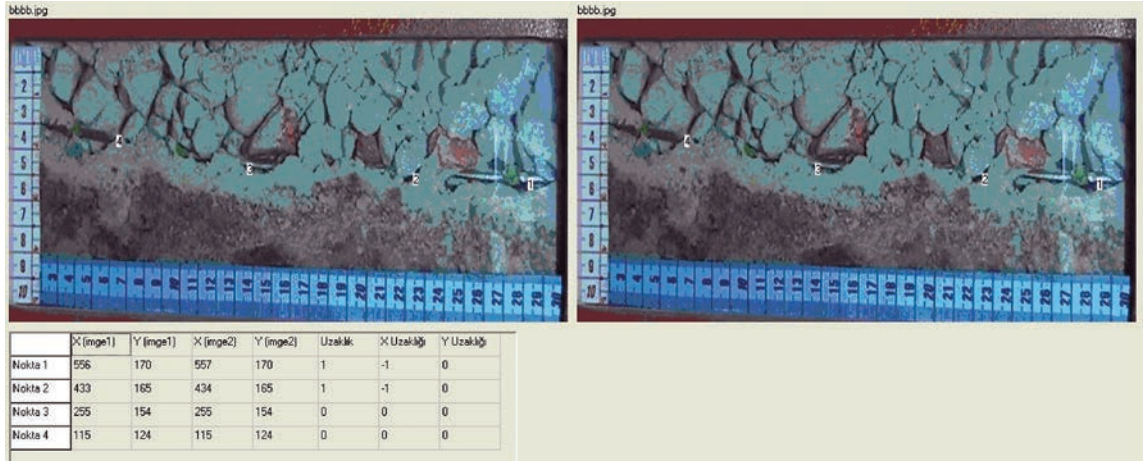

Fig. 7. Initial (left) and final image (right) and the immediate displacement values. The first photo is obtained at the beginning of the test and the second one is obtained at the end of the test

Table 3. Vertical stress distribution

Geogrid types	Test No.	Bottom of geogrid level, kPa				Average	Standard deviation	Top of geogrid level, kPa				Average	Standard deviation
		Sensor No.						Sensor No.					
		1	2	3	4			5	6	7	8		
50×50 mm	1	91	14	27	64	49	35.1	113	18	13	39	45.75	46.2
	2	54	39	17	56	41.5	18.01	63	73	4	29	42.25	31.7
	3	14	5	16	34	17.5	12.1	22	31	14	75	35.5	27.23
	Average	53	19.3	20	51.33	36	21.73	66	40.6	10.3	47.67	41.16	35.04
40×40 mm	1	5	17	21	40	20.75	14.5	1	2	3	53	14.75	25.51
	2	31	13	16	18	19.5	7.9	25	16	17	9	16.75	6.55
	3	26	19	32	13	22.5	8.26	40	41	16	66	40.75	20.41
	Average	20.6	16.3	23	23.67	20.91	10.22	22	19.6	12	42.67	24.08	17.49
30×30 mm	1	5	6	19	–	10	7.81	5	7	11	–	7.66	3.05
	2	17	3	65	26	27.75	19.7	2	11	109	101	55.75	57.08
	3	7	16	36	17	19	12.19	155	11	20	31	54.25	67.6
	Average	9.66	8.33	40	21.5	18.91	13.23	54	9.66	46.7	66	39.22	42.57

50×50 mm aperture size geogrid levels, it could be seen that at the top of geogrid level average vertical pressure value of all test numbers and all sensors was 16% higher than those of bottom geogrid level. Similarly, standart deviation value at top level was 66% higher than at bottom level. According to Table , in the event of using 40×40 mm aperture size geogrid, the average vertical pressure of top of the geogrid level was 1.2 times and standart deviation was 1.7 times higher than those of bottom of the geogrid level. For 30×30 mm aperture size geogrid, at the top of geogrid level vertical pressure value was almost 2 times higher than the stress value at the bottom of geogrid and standart deviation was 3 times higher than standart deviation of bottom of the geogrid level. For test number 1 the stresses measured by sensors 5, 6, 7, and 8 located at the top of 40×40 mm aperture size geogrid was calculated as 14 kPa which was almost 14 times higher than the stress value of 1 kPa at the test number 1 the stress measured by sensor 1. For test number 1 the stresses measured by sensor 5, 6 and 7 located at the top of 30×30 mm aperture size geogrid, stress values obtained from sensors and their average value were comparatively adjacent. According to these determinations, it is worth saying that the vertical stress distribution composed at different level in pullout box was non-uniform.

3.3. Wide-width tensile test results

Further experimental analysis was conducted on the same samples to investigate the wide-width tensile strength properties. Wide-width tensile tests of the longitudinal ribs were performed with unconfined geogrid specimens based on the ASTM standard *Standart Test Method for Tensile Properties of Geotextiles by the Wide-width Strip Method*. Table 4 shows the wide-width tensile test results for all geogrid samples tested. The results for 30×30 mm geogrid aperture size indicate average tensile strength of 3.42 kN/m and max elongation of 10%. Larger values were observed for 50×50 mm aperture size geogrid (5.7 kN/m and 10%, respectively). Using the tensile peak strength results, it was checked that tensile strength properties of the 50×50 mm aperture size geogrids were better than those of 40×40 mm (2.68 times higher) and 30×30 mm (1.95 times higher) aperture size geogrids. Comparison of the test results showed that unconfined geogrid wide-width tensile strengths were about the same as that obtained from pullout strength tests per unit width as shown in Table 3. The wide-width tensile strength values of geogrids were about 0.1 kN/m to 1 kN/m lower than their pullout strength strength values per unit width. In the case of 50×50 mm type geogrids, the extra pullot strength values were 1 N/m above the wide-width tensile strength values. The differences between the pullout and wide-width test results are due to the difference in clamping mechanisms, unconfinement, and unconfinement conditions.

According to statistical analyses on tensile test results shown in Table 4, for three types of geogrids (50×50 mm, 40×40 mm, 30×30 mm) standart deviation of peak strength value was lower than residual strength value. On the contrary, in pullout tests standart deviation of peak strength value was higher than residual strength value. In the pullout tests, standart deviation values were not small and probably it was due to interlocking with geogrid and soil particle. Soil material properties, aggregate dimensions and surface friction state can be effective parameters in this regard.

As demonstrated by this study, it was found that geogrids are unique in their pullout performance within pavement subbase layer structure based on their aperture sizes. These findings throw light on the relative importance of geogrid aperture size in pullout performance tests, but they should be viewed with a caution due to the lack of historic data on additional factors affecting long-term field subbase-subgrade layer performance of asphalt pavements.

4. Conclusions

The findings of this study are limited to laboratory tests. It is possible that these findings may vary if conducted on the field for long term subbase-subgrade pavement layer performances. The main conclusions concluded from this study are:

1. All three geogrid types showed almost no lateral displacement. The lateral displacement of the subbase is prevented and the geogrid is successful in confining the subbase layer and subgrade soils. It is clear that high resistance to permanent deformation of subbase layer can be achived by stiff ribs providing interlock of soil particles into the aperture.

Table 4. Pullout and wide width tensile strength values of the geogrid samples

	Aperture size geogrid														
	50×50 mm					40×40 mm					30×30 mm				
	Test No.			Average	Std. dev.	Test No.			Average	Std. dev.	Test No.			Average	Std. dev.
	1	2	3			1	2	3			1	2	3		
	Tensile test, kN/m														
Peak	5.64	5.76	5.76	5.72	0.05	2.8	2.72	2.64	2.71	0.08	3.52	–	3.32	3.42	0.14
Residual	3.1	5.1	3.4	3.86	0.88	2.1	1.9	1.65	1.88	0.22	2.9	–	2.5	2.7	0.28
	Pullout test, kN/m														
Peak	7.76	6.56	5.66	6.66	0.86	3.04	2.4	2	2.48	0.52	3.2	3.6	3.36	3.38	0.2
Residual	4.2	3.9	3	3.7	0.5	1.8	1.3	1.1	1.4	0.36	1.55	1.45	1.23	1.41	0.163

2. Pressure sensors installed on top and bottom of the geogrid samples indicated that the geogrids reduce the vertical stress significantly by distrubuting the vertical load to a wide range over the subgrade soil. The reduction in the vertical stress on top of the subgrade was 12%, 14%, 52% for 50×50 mm, 40×40 mm, and 30×30 mm aperture size geogrids, respectively. This important finding indicates that smaller aperture size geogrids can improve the subgrade bearing capacity in terms of vertical stresses.
3. The pullout peak strength values for all types of geogrids were calculated as 6.66 kN/m, 2.48 kN/m, 3.38 kN/m for 50×50 mm, 40×40 mm, 30×30 mm aperture size geogrids, respectively. The 50×50 mm aperture size geogrid has given ideal results in terms of the pullout force. The aperture structure of a 50×50 mm geogrid exhibits the highest mutual effect with the surrounding subbase soil, and this characteristic allows the geogrid to be used as a prime reinforcement for subbase structures.
4. The mechanical ultimate strain values were measured as 24%, 17%, 20% for 50×50 mm, 40×40 mm, 30×30 mm aperture size geogrids, respectively, and also peak strain values were measured as 10%, 5% and 13.5% for 50×50 mm, 40×40 mm, 30×30 mm aperture size geogrids, respectively.
5. According to the results of wide-width tensile tests, peak tensile strength properties of the 50×50 mm aperture size geogrids were better than those of 40×40 mm (2.68 times higher) and 30×30 mm (1.95 times higher) aperture size geogrids. This is due to the fact that the 50×50 mm aperture size geogrids had the highest elongations of 10%.
6. Comparison of the test results showed that unconfined geogrid wide-width tensile strengths were about the same as that obtained from pullout strength tests per unit. The wide-width tensile strength values of geogrids were about 0.1 kN/m to 1 kN/m lower than their pullout strength values per unit width.
7. It was found that strains at failure observed during tensile tests were roughly of the same magnitude as those at failure during the pullout shear strength tests.

Acknowledgements

This study is funded by TÜBİTAK under grant project No. 106M423 and KTÜ BAP. This support is gratefully acknowledged.

References

Alagiyawanna, A. M. N.; Sugimoto, M.; Sato, S.; Toyota, H. 2001. Influence of Longitudinal and Transverse Members on Geogrid Pullout Behaviour During Deformation, *Geotextiles and Geomembranes* 19(8): 483–507. http://dx.doi.org/10.1016/S0266-1144(01)00020-6

Alamshahi, S.; Hataf, N. 2009. Bearing Capacity of Strip Footings on Sand Slopes Reinforced with Geogrid and Grid-Anchor, *Geotextiles and Geomembranes* 27(3): 217–226. http://dx.doi.org/10.1016/j.geotexmem.2008.11.011

Abusharar, S. W.; Zheng, J.-J.; Chen, B.-G.; Yin, J.-H. 2009. A simplified method for analysis of a piled embankment reinforced with geosynthetics, *Geotextiles and Geomembranes* 27: 39–52. http://dx.doi.org/10.1016/j.geotexmem.2008.05.002

Cancelli, A.; Montanelli, F. 1999. In-ground Test for Geosynthetic Reinforced Flexible Paved Roads, in *The Conference "Geosynthetics'99: Specifying Geosynthetics and Developing Design Details"*, vol. 2. April 28–30, Boston, Massachusetts, USA. 863–879.

Dong, Y.-L.; Han, J.; Bai, X.-H. 2011. Numerical Analysis of Tensile Behavior of Geogrids with Rectangular and Triangular Apertures, *Geotextiles and Geomembranes* 29(2): 83–91. http://dx.doi.org/10.1016/j.geotexmem.2010.10.007

Dong, Y. L.; Han, J.; Bai, X. H. 2010. Bearing Capacities of Geogrid-Reinforced Sand Bases under Static Loading, in *Proc. of the GeoShanghai 2010 International Conference*. June 3–5, 2010, Shanghai, China. Ground Improvement and Geosynthetics. Geotechnical Special Publication No. 207. Ed by Puppala, A. J.; Huang, J.; Han, J.; Hoyos, L. R. 275–281.

Ghosh, C.; Madhav, M. R. 1994. Reinforced Granular Fill-Soft Soil System: Membrane Effect, *Geotextiles and Geomembranes* 13(11): 743–759. http://dx.doi.org/10.1016/0266-1144(94)90061-2

Fang, H.; Hand, A. J.; Haddock, J. E., White, T. D. 2007. An Object-Oriented Framework for Finite Element Pavement Analysis, *Advances in Engineering Software* 38(11–12): 763–771. http://dx.doi.org/10.1016/j.advengsoft.2006.08.045

Jewell, R. A. 1990. Reinforcement Bond Capacity, *Geotechnique* 40(3): 513–518. http://dx.doi.org/10.1680/geot.1990.40.3.513

Kongkitkul, W.; Tatsuoka, F.; Hirakawa, D.; Sugimoto, T.; Kawahata, S.; Ito, M. 2010. Time Histories of Tensile Force in Geogrid Arranged in Two Full-Scale High Walls, *Geosynthetics International* 17(1): 12–33. http://dx.doi.org/10.1680/gein.2010.17.1.12

Lopes, M. L.; Ladeira, M. 1996. Influence of the Confinement, Soil Density and Displacement Rate on Soil–Geogrid Interaction, *Geotextiles and Geomembranes* 14(10): 543–554. http://dx.doi.org/10.1016/S0266-1144(97)83184-6

Moraci, N.; Mandaglio, M. C.; Ielo, D. 2012. A New Theoretical Method to Evaluate the Internal Stability of Granular Soils, *Canadian Geotechnical Journal* 49(1): 42–58. http://dx.doi.org/10.1139/t11-083

Moraci, N.; Gioffrè, D. A. 2006. Simple Method to Evaluate the Pullout Resistance of Extruded Geogrids Embedded in a Compacted Gronuler Soil, *Geotextiles and Geomembranes* 24(2): 116–128. http://dx.doi.org/10.1016/j.geotexmem.2005.11.001

Mulungye, R. M.; Owende, P. M. O.; Mellon, K., 2007. Finite Element Modelling of Flexible Pavements on Soft Soil Subgrades, *Materials and Design* 28(3): 739–756. http://dx.doi.org/10.1016/j.matdes.2005.12.006

Palmeira, E. M.; Antunes, L. G. S. 2010. Large Scale Tests on Geosynthetic Reinforced Unpaved Roads Subjected to Surface Maintenance, *Geotextiles and Geomembranes* 28(6): 547–558. http://dx.doi.org/10.1016/j.geotexmem.2010.03.002

Palmeira, E. M. 2009. Soil–Geosynthetic Interaction: Modelling and Analysis, *Geotextiles and Geomembranes* 27(5): 386–390. http://dx.doi.org/10.1016/j.geotexmem.2009.03.003

Palmeira, E. M. 2004. Bearing Force Mobilisation in Pull-Out Tests on Geogrids, *Geotextiles and Geomembranes* 22(6): 481–509. http://dx.doi.org/10.1016/j.geotexmem.2004.03.007

Palmeira, E. M.; Milligan, G. W. E. 1989. Scale and other Factors Affecting the Results of Pull-Out Tests of Grid Buried in Sand, *Géotechnique* 39(3): 511–524. http://dx.doi.org/10.1680/geot.1989.39.3.511

Park, D.-W. 2008. Prediction of Pavement Fatigue and Rutting Life Using Different Tire Types, *KSCE Journal of Civil Engineering* 12(5): 297–303. http://dx.doi.org/10.1007/s12205-008-0297-4

Perkins, S. W. 1999. Mechanical Response of Geosynthetic Reinforced Flexible Pavements, *Geosynthetics International* 6(5): 347–382.

Phanikumar, B. R.; Prasad, R.; Singh, A. 2009. Compressive Load Response of Geogrid-Reinforced Fine, Medium and Coarse Sands, *Geotextiles and Geomembranes* 27(3): 183–186. http://dx.doi.org/10.1016/j.geotexmem.2008.11.003

Priest, A. L.; Timm, D. H.; Barrett, W. E. 2005. *Mechanistic Comparison of Wide-Base Single Versus Standard Dual Tire Configurations*. NCAT Report 05-03.

Rowe, R. K.; Taechakumthorn, C. 2011. Design of Reinforced Embankments on Soft Clay Deposits Considering the Viscosity of Both Foundation and Reinforcement, *Geotextiles and Geomembranes* 29(5): 448–461. http://dx.doi.org/10.1016/j.geotexmem.2011.03.001

Sert, T.; Akpinar, M. V. 2011. Investigation of Geogrid Performance on Highway Subbase by Using the Pullout Test Device, *Technical Journal of Turkish Champer of Civil Engineers* 22(1): 5285–5304.

Subaida, E. A.; Chandrakaran, S.; Sankar, N. 2009. Laboratory Performance of Unpaved Roads Reinforced Withwoven Coir Geotextiles, *Geotextiles and Geomembranes* 27(3): 204–210. http://dx.doi.org/10.1016/j.geotexmem.2008.11.009

Sugimoto, M.; Alagiyawanna, A. M. N.; Kadoguchi, K. 2001. Influence of Rigid and Flexible Face on Geogrid Pullout Tests, *Geotextiles and Geomembranes* 19(5): 257–328. http://dx.doi.org/10.1016/S0266-1144(01)00011-5

Teixeira, S. H. C.; Bueno, B. S.; Zornberg, J. G. 2007. Pullout Resistance of Individual Longitudinal and Transverse Geogrid Ribs, *Journal of Geotechnical and Geoenvironmental Engineering* 133(1): 37–50. http://dx.doi.org/10.1061/(ASCE)1090-0241(2007)133:1(37)

Wu, Z. 2007. Evaluating Structural Performance of Base/Subbase Materials at the Louisiana Accelerated Pavement Research Facility, in *Proc. of International Conference on Transportation Engineering 2007*. February 11–14, 2007, Baton Rouge, Louisiana, USA.

Yeo, S. S.; Hsuan, Y. G. 2010. Evaluation of Creep Behavior of High Density Polyethylene and Polyethylene-Terephthalate Geogrids, *Geotextiles and Geomembranes* 28(5): 409–421. http://dx.doi.org/10.1016/j.geotexmem.2009.12.003

Received 13 September 2010; accepted 13 September 2011